

Characteristic analysis MIM waveguide amplifier by SPASER technology

Zhu Jun¹, Qin Liuli², Song Shuxiang¹

(1. College of Electronic Engineering, Guangxi Normal University, Guilin 541004, China;

2. College of Mathematics and Statistics, Guangxi Normal University, Guilin 541004, China)

Abstract: At present, SPASER (Surface Plasmon Amplification by Stimulated Emission of Radiation) is the smallest nanoscale active device, which is the first to function under visible light. In this paper, the MIM (metal-insulator-metal) waveguide structure of a double steady state was designed, which introduces the SPASER technology, namely, the surface plasmon wave amplifier. The amplifier was obtained by deriving from the Bloch equation using the SPASER laser theory. When the pumping rate was less than the threshold value, the number of the gain medium inversion particles remained 0. Otherwise, the number of the inversion particle grew linearly. The geometrical characteristics of the system could be completely described by the eigenmode function. On the central eigenmode, the system property entirely depended on the material parameters. Choosing the appropriate material parameters could make each state of the relaxation characteristic time remain at the level of the picosecond magnitude. The calculated results of the model show that the improved structure does not change the strong localized characteristics of the SPPs (Surface Plasmon Polaritons). The device solves the limitation on the surface plasmon net profit elimination caused by SPASER internal feedback.

Key words: surface plasmon; stimulated radiation amplification; pump rate;
inversion of particle number

CLC number: O23 **Document code:** A **DOI:** 10.3788/IRLA201645.0320002

SPASER 技术的 MIM 波导放大器特性分析

朱 君¹, 秦柳丽², 宋树祥¹

(1. 广西师范大学 电子工程学院, 广西 桂林 541004;

2. 广西师范大学 数学与统计学院, 广西 桂林 541004)

摘 要: SPASER 是所报道的最小的、第一个在可见光或更宽的波长范围内工作的纳米级的有源器件。采用双稳态方法, 将 SPASER 技术引入到改进的 MIM 波导结构实现表面等离子波放大器设计, 理论上采用 SPASER 的激光理论的 Bloch 方程推导得出: 泵浦速率小于阈值时, 增益介质反转粒子数保持为 0, 在泵浦速率大于阈值时, 反转粒子数随泵浦速率线性增长; 系统的几何特性完全由本征模式函数描述, 在给定本征模式下, 其性质完全取决于材料参数; 选择合适的材料参数, 可以使各状态的驰豫特征时间都在亚皮秒量级。模型计算结果表明: 改进结构不会改变 SPPs 的强局域化特性; 器件

收稿日期: 2015-07-05; 修订日期: 2015-08-20

基金项目: 国家自然科学基金(61361011); 广西自然科学基金(2015GXNSFBA139257);

广西师范大学重点项目(2015ED03); 广西自动检测技术与仪器重点实验室(YQ16206)

作者简介: 朱君(1985-), 男, 硕士生导师, 博士, 主要从事微纳器件设计与制作方面的研究。Email: zhujun1985@gxnu.edu.cn

解决了 SPASER 内反馈造成的表面等离子净增益消除的难题。研究成果可应用到生物传感、波谱检测、显微成像、超快通信等领域。

关键词: 表面等离子; 受激辐射放大; 泵浦速率; 反转粒子数

0 Introduction

In optical resonance nonlinear characteristics, a disordered structure expands to an orderly multilayer membrane structure. A composite medium with high volume fraction, which is a material orderly nanometal particles and nonlinear optical resonance, shows the progress in chromatophore studies^[1-3]. In 2010, Science published an article entitled the nanometer laser is the smallest excitation device (Nanolasers Smallest of the Small). In this challenging paper, SPASER research was described and summarized. A creative theoretical model and experimental method are introduced and a prospect for the developmental trend is presented. To date, in the study of micro/nanostructured amplifiers, the SPASER is the smallest nanoscale active device reported, which is the first device in this scale that works in the visible light or in a wide range^[4-7]. The SPASER technology essentially involves the principle of limited ion-metal particles and photons resonating in semiconductor media, which results in energy switching and amplification in an extremely small space. The minimum radius of the local spatial scope is 1 nm, while the depth of penetration of a nanoplasmon can reach 25 nm (medium surfacial depth)^[8-9]. Based on this theory, the research and design of a nanoquantum generator and super fast amplifier from the UV to the infrared range is no longer a scientific idea but has emerged as a frontier in science and technology^[10-11]. SPASER is a new research field that combines super feeling, super intensive and super fast metamaterials (perfect lens, super lens, negative refraction materials, left-handed materials, and the invisibility cloak)^[12-14]. The theory of SPASER technology starts

from the electromagnetically distributed ion and photon and is considered from the periodic vibration in the metal surface plasmon and stimulated photon resonant mode. The points that should be considered are the choice of the laser mode and competition, even the magnified feedback that is offered by the limited ion surface resonance of the free electrons in the metal particle, so that a coherent plasmon field can be formed^[15-17]. The SPASER can be formed from a surface plasmon by generating laser and amplifying photon. This concept was first collaboratively introduced by the Georgia State University (USA) and the University of Tel Aviv in 2003. The SPASER experiments have been demonstrated by the Purdue University and Norfolk State University in 2009. Noginov and from the Norfolk State University presented a paper that has been recognized as one of the ten most focused papers in "Nature" because of its creativity; this academic paper is the core of the present experiment^[18]. From the physical principle, metal plasmon nanoparticles on the surface of a plasmon model will cause internal feedback. This feedback occurs because the surface plasmon mode changes periodically in the gain medium, and this behavior is difficult to fundamentally eliminate. This phenomenon will cause the saturation of the SPASER gain, which leads to the SPASER pure magnification coefficient to become zero in the fixed condition. This characteristic determines that the SPASER cannot be made into an amplifier. Extensive studies have been performed to resolve this limitation, and two techniques have been determined to make the SPASER into a nanoamplifier. One method is the dynamic(transient) method, in which the SPASER will have a zero net

amplification coefficient before it goes through a femtosecond transient process. This process is performed after the population inversion and before the continuous wave is determined. Another technique is the bistable method, which is improved by Bloch equations of the laser theory of SPASER on the basis of mixing the saturated absorber in the gain medium. Theoretically, this method can use the SPASER to develop the bistable super fast nanoamplifier. In this study, the second technique is used to fabricate a SPASER amplified waveguide device. The results can be applied to biological sensing, spectrum detection, microscopic imaging, super-fast communication, etc.

1 Theoretical model analysis of bistable amplifier

A theoretical description of the structure(Fig.1) is presented, which includes the ordinary and the improved MIM waveguide structures.

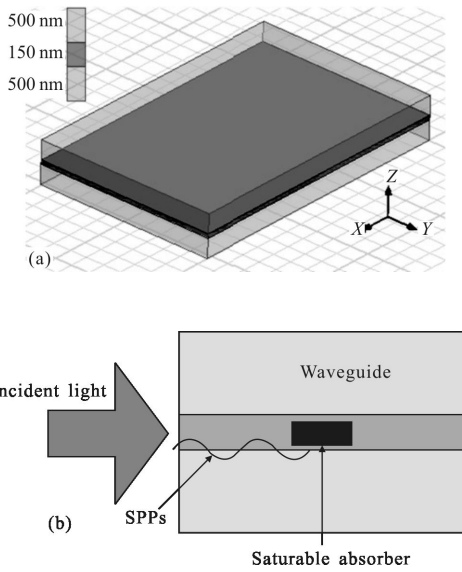


Fig.1 Ordinary MIM waveguide structure

Figure 1(a) is the ordinary MIM waveguide structure; Figure 1 (b) is the improved MIM waveguide structure based on the theory of optical Bloch equations, the basic parameter equations for SPASER are as follows:

$$\dot{\rho}_{12}^{(p)} = -[i(\omega_s - \omega_{21}) + \Gamma_{12}] \rho_{12}^{(p)} + i a_{0n} n_{21}^{(p)} \tilde{\Omega}_{12}^{(p)} \quad (1a)$$

$$\tilde{\Omega}_{12}^{(p)} = - \left(\frac{4\pi \hbar s_n}{\epsilon_1 \epsilon_0 \epsilon_n'} \right)^{1/2} \frac{\vec{d}_{12}^{(p)} \cdot \nabla \phi_n(r_p)}{\hbar} \quad (1b)$$

$$\dot{n}_{21}^{(p)} = -4\text{Im}[a_{0n} \rho_{12}^{(p)} \tilde{\Omega}_{12}^{(p)}] - \gamma_2(1+n_{21}^{(p)}) + g(1-n_{21}^{(p)}) \quad (1c)$$

$$\dot{a}_{0n} = [i(\omega_s - \omega_n) - \gamma_n] a_{0n} + i \sum_p \rho_{12}^{(p)*} \tilde{\Omega}_{12}^{(p)} \quad (1d)$$

where a_{0n} is the slowly varying amplitude of eigenmode ϕ_n . $\rho_{12}^{(p)}$ and $n_{21}^{(p)}$ are the density matrix of transition and population inversion for the p th chromatophore, respectively. g is the pump rate of the gain medium. $\tilde{\Omega}_{12}^{(p)}$ is the frequency of the single excimer Rabi for the p th chromatophore. $d_{12}^{(p)}$ is the corresponding dipole transition yuan. Constant Γ_{12} describes the polarization relaxation, and γ_n is the line width of the eigenmode.

$$\omega_s = \frac{\gamma_n \omega_{21} + \Gamma_{12} \omega_n}{\gamma_n + \Gamma_{12}} \quad (2)$$

The above equation is the SPASER transmission frequency. First, the characteristics of the equivalent SPASER steady-state should be investigated under different transmission frequencies. The waveguide width is $d=0.5 \mu\text{m}$, and the dielectric function of silver is obtained from the literature. Additionally, $\hbar\Gamma_{12}=0.02 \text{ eV}$, $\hbar(\omega_s - \omega_n)=0.02 \text{ eV}$, and the gain medium density is $2.4 \times 10^{23} \text{ m}^{-3}$.

The simulation results are shown in Figure 2, which reflects the change in the SPP excimer and gain medium population inversion with increasing pump rate. The excitation curves under the different frequencies exhibit pump rate threshold values. When the pump rate is less than the threshold value, N_n remains at 0, and n increases linearly with g . When the pump rate is higher than the threshold value, N_n grows linearly with the pump rate, and n is at a low level. The threshold value of high-frequency SPASER is lower because its photon energy is larger, and the disturbance of the spontaneous radiation noise to stimulated radiation model is stronger. Compared with the structure of nanoparticles, the increasing system volumes result in higher number of excimers in the SPASER waveguide structure. However, the particle

inversion level is higher, because the photon level is lower. The results from the different waveguide widths and depths show that, in addition to the change in geometric shape that influences the eigenmode function, the excitation curve of SPASER is not affected by geometric factors, especially by the waveguides of different depths. Hence, the systematic geometrical characteristic is completely described by the eigenmode function. At a certain eigenmode, the character is completely dependent on the material parameter. Then, we mix a saturable absorber in the gain medium so that the SPASER will exhibit bistable characteristics.

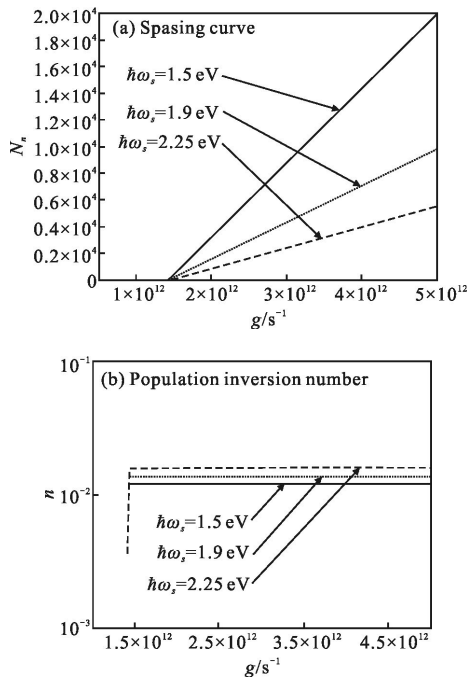


Fig.2 MIM waveguide on different frequencies

The form of the optical Bloch equation containing a saturated absorber is similar to Eq. (1). Only the index p considers the number of gain medium chromatophore and saturable absorber simultaneously, and on Eq. (1c) of the saturated absorber, the pump rate is $g=0$.

From Figure 3, when the density of the saturated absorber is 0.3 times the gain medium density, $\hbar\omega_s=1.5$ eV represents the curve that corresponds to the inverted population, the solid line refers to the branch of $N_n=0$, and the dotted line corresponds to the branch

of N_n . The job characteristics of the bistable SPASER are considered under the condition of a pulse pump. When $t=0$, the system suddenly obtains the pump,

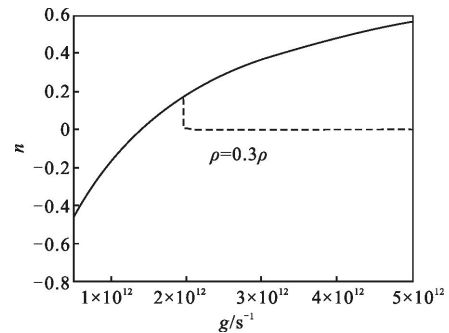


Fig.3 Population inversion number of bistable SPASER

then the changes in the system depends on the value of N_n at $t=0$. Figure 4 shows the simulation result, in which $d=0.5 \mu\text{m}$ is the waveguide of the working frequency, $\hbar\omega_s=1.5$ eV is the nanocavity ($\rho_s=0.3\rho$ and $g=5 \times 10^{12} \text{s}^{-1}$). Figure 4(a) shows that when N_n is initially higher, the system achieves a high bistable state during a series of rapid oscillations until the pump exists, and the characteristic time is approximately hundreds of femtosecond. Figure 4 (b) shows that when N_n is initially lower, the system at 100 fs quickly relaxes to 0. Figure 4 uses the logarithmic

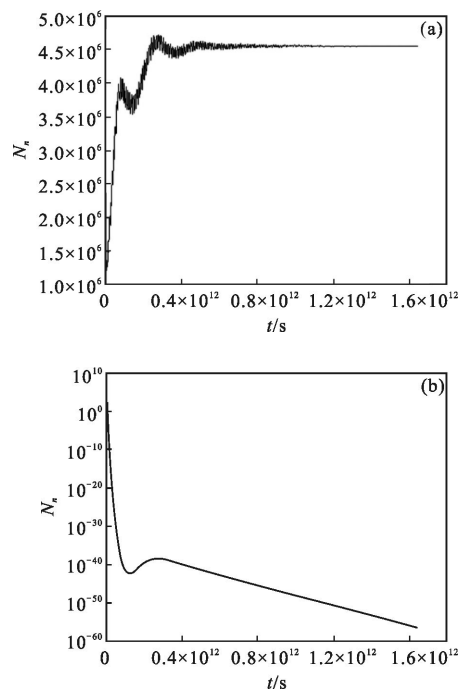


Fig.4 SP population N_n of bistable SPASER

coordinate. The initial N_n shows the threshold value, which is divided into the aforementioned two kinds of conditions. This critical value is also used as an amplifier of the threshold. Therefore, a bistable of the waveguide structure equivalent SPASER can be used as digital signal amplifier under the condition of a pulse pump. If it transmits SPP square wave signals in the MIM waveguide, under type (2), when the signal "1" transmits to the SPASER structure, the number of the internal nanophoton in the cavity increases. If the system has pumps, the signal photons will become the SPASER initial N_n . If the initial N_n is over the critical value, the photon number in the system will increase rapidly to the bistable state N_n values. The output of the system increases corresponding, that is, the signal amplitude is amplified. At the end of the pulse pump, the system relaxes to 0, and the output decreases. When signal "0" is transmitted to the SPASER, even in the presence of a pump, given the insufficient initial N_n , the system remains in a bistable low state, and it will not produce an amplified signal output.

The SPASER bistable amplifier is a typical threshold amplifier. The amplifier threshold is determined by the initial threshold under the pressure of a given pump rate. The threshold level is related to the density of the saturable absorber chromatophore. In addition, it is also related to the eigenmode volume of the system pattern. Another significant feature of the SPASER amplifier is its super fast characteristic. Considering the system optical Bloch equations, the parameters related to the characteristics include the detuning $\omega_{12}-\omega_n$, the gain medium Γ_{12} of the relaxation factor, and the eigenmode line width γ_n . These parameters can be determined by the nature of the material. Selecting the appropriate material parameters can make the relaxation characteristic time of each state remain at the picosecond magnitude.

2 Calculated results

2.1 FDTD analysis

Thus, SPASER can be used for super fast

amplification in picoseconds. The application of a picosecond pulse signal is highly significant for an ultra-high-speed information processing system.

Figure 5 shows that the FDTD should be analyzed first for the designed amplifier. The E_x and H_y of the waveguide structure has good restrictiveness. A very strong field distribution is found at the corner of the metal apex caused by the edge effects at this position. Given the presence of large amounts of bound charge in the edge area, the original field strength is improved significantly throughout the collective shock excitation of the surface plasmon. Results show that this kind of waveguide structure does not change the localized features of the SPPs. Thus, an amplifier device structure is feasible.

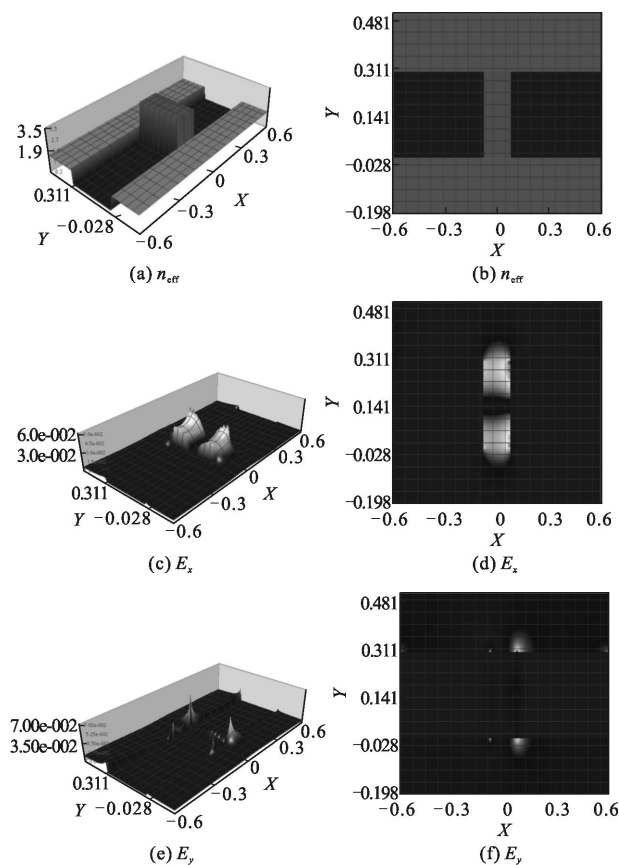


Fig.5 Distribution of electromagnetic field on the XY plane

2.2 Analysis on number of plasmon excitons results

With the aforementioned experimental scheme and contents, Figure 6 shows the number of the

plasmon excitons, which is under three different conditions, such as transient high state, low state, and without the embedded saturable absorber, by adopting the improved MIM waveguide structure of the SPASER amplifier. From Figure 6, when the number of the initial surface plasmon N_n is less than the critical value (Figure 6 (a)), a series of relaxation oscillation is presented. The relaxation of SPASER increases rapidly with $N_n \rightarrow 0$. This phenomenon is determined by enhancing the energy conversion to the metal surface plasmon mode. When the initial value is N_n , the number of initial plasmon surface excitons is large enough, because of the relaxation oscillation. In less than 100 fs, the number of initial value will be attained. Thus, theoretically, the number of initial plasmon surface excitons reaches a stable level. After reaching the steady state, the number will remain at this state for a long time. The analytical result of the spreading of the common MIM structure SPPs (Figure 6 (c)) shows that the number of the initial surface exciton plasmon also increases. However, under continuous pumping, a large number of excitons will not be exported until the process tends to be zero. The experimental results show that the device solves the plasmon net profit wiping caused by SPASER internal feedback.

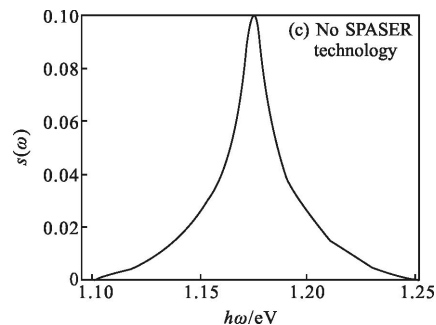
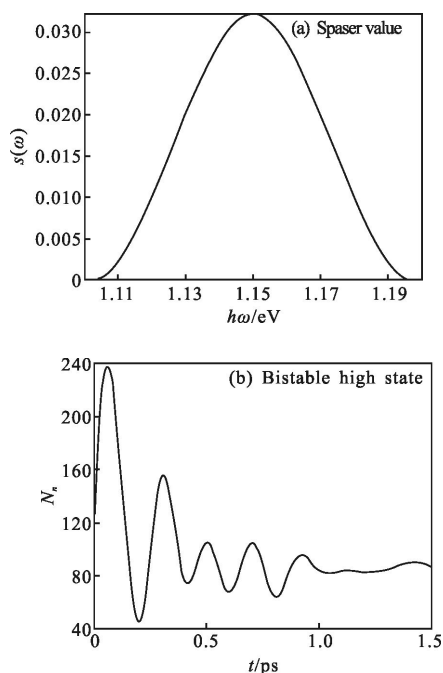


Fig.6 Number of the plasmon excitons

3 Conclusion

A surface plasmon amplifier has been developed based on the SPASER mechanism. This amplifier is theoretically analyzed using the density matrix equation. The MIM waveguide structure with a saturable absorber is used in surface plasmon amplifier. The realized metal thin-film technology is used to fabricate the amplifier, and the pulse response time of the designed amplifier reaches 100 fs. Results from this study on the SPASER amplification device will be uniquely applied in the transmission and storage of information, control of laser beam, photoelectric super-fast conversion, control of photon, electric pump light source at the nanoscale level, small laser plasmon, and so on.

References:

- [1] Stiles P L, Dieringer D J, Shah N C, et al. Surface-enhanced Raman spectroscopy [J]. *Ann Rev Anal Chem*, 2008, 1: 601–626.
- [2] Anker J N, W Paige H, Ulga L, et al. Biosensing with plasmonic nanosensors [J]. *Nature Mater*, 2008, 7 (6): 442–453.
- [3] Homola J. Surface plasmon resonance sensors for detection of chemical and biological species [J]. *Chem Rev*, 2008, 108: 462–493.
- [4] Bergman D J, Stockman M I. Surface plasmon amplification by stimulated emission of radiation: quantum generation of coherent surface plasmons in nanosystems [J]. *Phys Rev Lett*, 2003, 90: 027402.
- [5] Li K, Li X, Stockman M I, et al. Surface plasmon amplification by stimulated emission in nanolenses [J]. *Phys*

- Rev*, 2005, 71: 115409.
- [6] Protsenko I E, Uskov A V, Zaimidoroga O A, et al. Dipole nanolaser[J]. *Phys Rev A*, 2005, 71: 063812.
- [7] Stockman M I. Spasers explained [J]. *Nature Photon*, 2008, 2: 327–329.
- [8] Chang S W, Ni C Y A, Chuang S L. Theory for bowtie plasmonic nanolasers[J]. *Opt Express*, 2008, 16(14): 10580–10595.
- [9] Rosenthal A S, Ghannam T. Dipole nanolasers: a study of their quantum properties[J]. *Phys Rev A*, 2009, 79: 043824.
- [10] Gramotnev D K, Bozhevolnyi S I. Plasmonics beyond the diffraction limit[J]. *Nature Photon*, 2010, 4: 83–91.
- [11] Lawandy N M. Localized surface plasmon singularities in amplifying media[J]. *Appl Phys Lett*, 2004, 85: 5040–5042.
- [12] Stockman M I. The spaser as a nanoscale quantum generator and ultrafast amplifier[J]. *J Opt*, 2010, 12: 024004.
- [13] Noginov M A, Zhu G, Bahoura M, et al. Enhancement of surface plasmons in an Ag aggregate by optical gain in a dielectric medium[J]. *Opt Lett*, 2006, 31(20): 3022–3024.
- [14] Gordon J A, Ziolkowski R W. The design and simulated performance of a coated nano-particle laser[J]. *Opt Express*, 2007, 15(5): 2622–2653.
- [15] Quinten M, Leitner A, Krenn J R, et al. Electromagnetic energy transport via linear chains of silver nanoparticles[J]. *Opt Lett*, 1998, 23: 1331–1333.
- [16] Citrin D S. Plasmon-polariton transport in metal-nanoparticle chains embedded in a gain medium [J]. *Opt Lett*, 2006, 31: 98–100.
- [17] Thylén L, Holmstrom P, Bratkovsky A, et al. Limits on integration as determined by power dissipation and signal-to-noise ratio in loss-compensated photonic integrated circuits based on metal/quantum-dot materials [J]. *IEEE J Quant Electron*, 2010, 46(4): 518–524.
- [18] Noginov M A, Zhu G, Belgrave A M, et al. Demonstration of a spaser-based nanolaser [J]. *Nature*, 2009, 460(7259): 1110–1113.